

Microstructural characteristics of Al–20Si–2Cu–0.4Mg–1Ni alloy formed by rheo-squeeze casting after ultrasonic vibration treatment

WU Shu-sen¹, ZHONG Gu¹, AN Ping¹, WAN Li¹, H. NAKAE²

1. State Key Laboratory of Materials Processing and Die & Mould Technology,

Huazhong University of Science and Technology, Wuhan 430074, China;

2. Department of Materials Science and Engineering, Waseda University, Tokyo 169, Japan

Received 11 October 2011; accepted 21 November 2012

Abstract: A swash plate for air conditioning compressor of cars was formed by rheo-squeeze casting with semi-solid Al–Si alloy slurry prepared by ultrasonic vibration process, and the microstructure of this alloy was investigated. Besides the microstructures of primary Si particles and $\alpha(\text{Al})+\beta\text{-Si}$ eutectic phases, non-equilibrium $\alpha(\text{Al})$ particles or dendrites are discovered in the microstructure of the Al–20Si–2Cu–0.4Mg–1Ni alloy. Rapid cooling generated by squeeze casting process rather than the pressure is considered as the main reason for the formation of non-equilibrium $\alpha(\text{Al})$ phase. The sound pressurizing effect of ultrasonic vibration also enables the non-equilibrium $\alpha(\text{Al})$ phases to form above eutectic temperature and grow into non-dendritic spheroids in the process of semi-solid slurry preparation. Non-equilibrium $\alpha(\text{Al})$ phases formed in the hypereutectic Al–Si alloy with ultrasonic vibration treatment, consist of round $\alpha(\text{Al})$ grains formed above the eutectic temperature and a small amount of fine $\alpha(\text{Al})$ dendrites formed under the eutectic temperature. The volume fraction of primary Si particles is decreased significantly by the effect of ultrasonic vibration through increasing the solid solubility of Si atoms in $\alpha(\text{Al})$ matrix and decreasing the forming temperature range of primary Si particles. The average particle diameter and the volume fraction of primary Si particles in microstructure of the swash-plate by rheo-squeeze casting are 24.3 μm and 11.1%, respectively.

Key words: Al–Si alloy; hypereutectic; ultrasonic vibration; squeeze casting; non-equilibrium $\alpha(\text{Al})$; semi-solid slurry

1 Introduction

High silicon ($\text{Si}>18\%$) Al–Si alloys are considered to be an ideal candidate for making heat-resistant parts such as pistons of high speed engines, due to the superior performances of high specific strength, excellent wear resistance and corrosion resistance, as well as low coefficient of thermal expansion [1]. Generally, conventional cast hypereutectic Al–Si alloys present the usual microstructures with primary Si and $\alpha(\text{Al})+\beta\text{-Si}$ eutectic phases [2]. However, non-equilibrium $\alpha(\text{Al})$ dendrites were found in die-casting [3] or squeeze casting [4] hypereutectic Al–Si alloys. The microstructure of high-pressure die-cast Al–20%Si alloy cylinder block was studied by YAMAGATA et al [4], and cooling rate was considered to change the morphology of non-equilibrium $\alpha(\text{Al})$ dendrites. The secondary dendrite arm spacing of non-equilibrium solidified $\alpha(\text{Al})$

decreased from $(22.1\pm 5.9) \mu\text{m}$ to $(5.1\pm 0.8) \mu\text{m}$ with the increase of cooling rate varied from 4.9 to 82.9 $^{\circ}\text{C/s}$. Even nearly spherical $\alpha(\text{Al})$ grains formed in hypereutectic Al–Si alloy were reported by BIROL [5] in thixotropic formed semi-solid Al–19.73%Si–2.84%Cu alloy. LASHKARI et al [6] in thixocasted A390 alloy. The granular $\alpha(\text{Al})$ grains played an important role in improving the properties of hypereutectic Al–Si alloys, such as toughness. The formation mechanism of non-equilibrium $\alpha(\text{Al})$ phase was generally considered the changes of phase diagram under high pressures by earlier study [7]. However, squeeze cast hypereutectic Al–Si alloys with the pressure less than 200 MPa also lead to the formation of non-equilibrium $\alpha(\text{Al})$ dendrites. Therefore, it is necessary to reveal the main reason that causes the formation of non-equilibrium $\alpha(\text{Al})$ phase.

In recent years, the rheological forming process with semi-solid slurry has attracted more and more attention for the merits as simple process, low cost,

and so on [8–11]. There are now many invented semi-solid rheoforming processes which are being studied or have been applied, such as electromagnetic stirring method, and sloping plate method [9,10]. The A356 alloy formed directly by rheo-squeeze casting of semi-solid slurry made with weak electromagnetic stirring method showed excellent mechanical properties [12]. Recently, ultrasonic vibration (USV) has been used to make semi-solid slurry, and for hypereutectic Al–Si alloy it has significant effects on refining the primary Si particles [13] and modifying the intermetallic compounds such as Fe-containing phase [14]. ZHAO et al [13] prepared semi-solid slurry of A390 alloy by USV process near the liquidus temperature. Fine primary Si particles about 20 μm in size were obtained in the A390 alloy.

In this work, an Al–20Si–2.0Cu–0.4Mg–1.0Ni alloy was produced by the combination of ultrasonic vibration treatment and rheological squeeze casting (RSC) process. The effects of squeeze casting (SC) and USV on the solidification of non-equilibrium $\alpha(\text{Al})$ phase were investigated. The difference of primary Si particles of this alloy was also compared between conventional SC and semi-solid SC processes.

2 Experimental

The installation of USV for preparing semi-solid slurry of high silicon Al–Si alloy in Ref. [13] was applied in this experiment. The applied ultrasonic power in this study was 1.8 kW, and the frequency of USV was 20 kHz. Ultrasonic vibrator composed of firmly connected transducer and amplitude made with titanium alloy.

The alloys used were Al–20Si–2Cu–0.4Mg–1Ni–0.5Mn (i.e. Al–20%Si alloy for short in the following, mass fraction, %), which were prepared by using raw materials of Al–25.8%Si and Al–10%Mn master alloy, commercially purity Al (99.7%), pure Cu (99.99%), pure Mg (99.9%), and pure Ni (99.99%). The final real compositions of the squeeze cast samples analyzed with fluorescent analyzer were 20%Si, 1.86%Cu, 0.314%Mg, 1.02%Ni, 0.214%Fe, 0.507%Mn, 0.24%Ce, 0.24%La, 0.047%Zn, 0.022%Ti, and balance Al. The liquidus and the solidus temperatures of this alloy determined by differential scanning calorimeter (DSC) were about 694 °C and 533 °C, respectively.

The alloy was melted in a resistance furnace at 820–850 °C with complex modification of 0.08%P (in the form of Cu–14%P) and 0.6%RE (in the form of Al–15%RE), in which the RE was composed of 63%Ce and 36%La. Then the melt was held at 740–780 °C, and a metal cup was preheated by the heating furnace simultaneously to about 690 °C. Subsequently, about

600 g liquid metal was poured into the preheated metal cup. The USV was applied to the melt with the ultrasonic vibrator immersed into the melt 15–20 mm in depth, when the liquid metal cooled down to about 710 °C. After the melt was treated with USV for 90 s at 710–690 °C, the slurry with a certain solid fraction was obtained. Then it was poured into the steel mold at 690 °C followed by rheo-squeeze casting (RSC) for producing a swash plate for air conditioning compressor of cars (Fig. 1) under the following parameters. Specific pressure was 120 MPa, injection speed was 50 mm/s, mold preheating temperature was about 200 °C, holding time of upper punch was 5–7 s, and that of lower punch was 12–15 s. For comparison, conventional squeeze casting samples were also made without USV treatment under the pouring temperature of 760 °C.

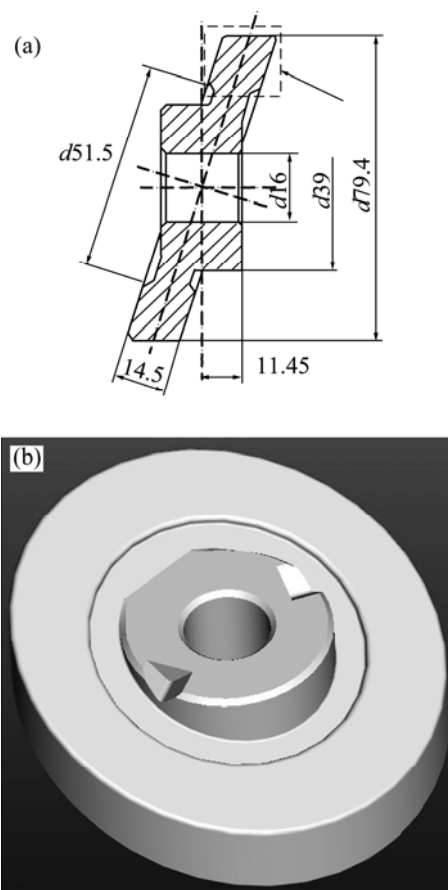


Fig. 1 Squeeze casting swash plate for air conditioning compressor of cars: (a) Simplified drawing; (b) 3D drawing (The arrow shows the sampling position.)

The part of the swash plate surrounded by the dashed line (Fig.1) was taken as metallographic sample. The microstructures of the polished specimens were revealed by etching with 0.5% hydrofluoric acid solution, and examined with an Axiovert 200MAT optical microscope. The volume fraction and average particle diameter (APD) of both $\alpha(\text{Al})$ phases and primary Si

particles were analyzed by image analysis software. In order to analyze the compositions, specimens were investigated by using Quanta 200 environmental scanning electron microscope (SEM) fitted with an energy dispersive X-ray spectroscopy (EDS) analysis system.

3 Results and discussion

3.1 Character of non-equilibrium $\alpha(\text{Al})$ phase in squeeze casting Al–20%Si alloy

Typical as-cast microstructures of this SC Al–20%Si alloy are shown in Fig. 2. The microstructures mainly consist of gray primary Si particles, white $\alpha(\text{Al})$ dendrites and fine $\alpha(\text{Al})+\beta\text{-Si}$ eutectic phases. The dark areas in Fig. 2(a) correspond to the eutectic microstructure which formed under rapid cooling condition. Based on the early studies [14], Mg_2Si , AlCuNi , and Al-Si-RE-Cu-Ni intermetallic compounds also existed in this alloy formed by conventional casting process. As shown in Fig. 2, most of the primary Si particles are surrounded by $\alpha(\text{Al})$ phases which appear in coarse dendrite or rosette-shape (directed by black arrow in Fig. 2). However, the equilibrium solidified phases of hypereutectic Al–Si alloy based on the Al–Si binary phase diagram only consist of primary Si and $\alpha(\text{Al})+\beta\text{-Si}$ eutectic phases, and there is no primary $\alpha(\text{Al})$ phase. Figure 3 shows the typical microstructure of gravity

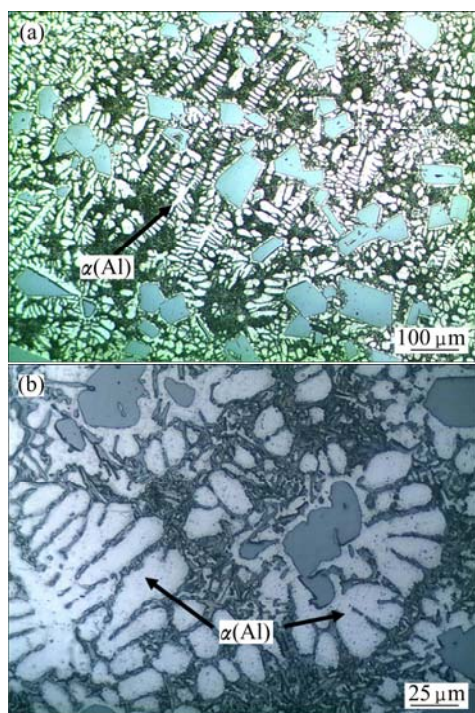


Fig. 2 Optical as-cast microstructures of Al–20%Si alloy by squeeze casting at 760 °C, indicating formation of non-equilibrium $\alpha(\text{Al})$ dendrites: (a) Low magnification; (b) High magnification

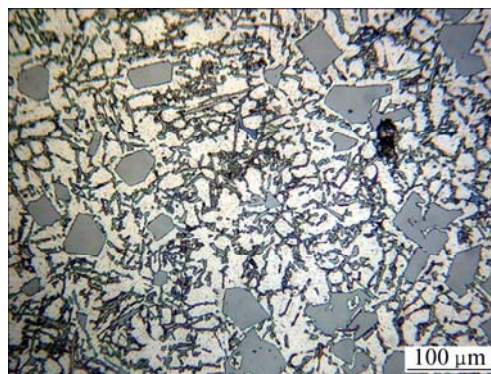


Fig. 3 Typical optical microstructure of gravity die-cast Al–20%Si alloy in as-cast state

die-cast Al–20%Si alloy which has similar microstructure of equilibrium solidified alloy. It presents clearly primary Si particles, and eutectics of $\alpha(\text{Al})$ and Si, in which there is no non-equilibrium $\alpha(\text{Al})$ dendrites.

Non-equilibrium $\alpha(\text{Al})$ phases of SC Al–20%Si alloy are supposed to correspond to the non-equilibrium solidification process under high pressure and rapid cooling condition. The application of pressure during solidification was expected to affect phase relationships in an alloy system. The eutectic point would move to the direction of higher Si contents and the temperature of eutectic point would rise up with the increase of pressure p [15]. It can be deduced by considering the Clausius–Clapeyron equation:

$$dT = \frac{T_m(V_2 - V_1)}{\Delta H_m} dp$$

where T_m is the equilibrium freezing temperature; V_2 and V_1 are the specific volumes of the liquid and solid alloy respectively; ΔH_m is the latent heat of fusion. The Si content of eutectic point was not over 20% until the pressure rose to 2.5 GPa, and the temperature of eutectic point was up to about 650 °C from 577 °C simultaneously. It has been proved experimentally that the liquidus temperature of Al–Si binary alloy only increased by 9 °C at 150 MPa [7]. Therefore, the slight effect can be caused by pressure application at 120 MPa on the liquidus temperature of Al–20%Si alloy. The rapid cooling rate which was produced in the SC process should be the dominant reason of the non-equilibrium solidification of $\alpha(\text{Al})$ dendrites. The following experiment is designed to provide evidence for this deduction. A copper mould as shown in Fig. 4 was used in this experiment. The mould prepared cylindrical samples with different diameters of 11, 14, 17 and 20 mm. The liquid metal was cast into the copper mold at 760 °C in order to keep the pouring temperature consistent with that of SC process.

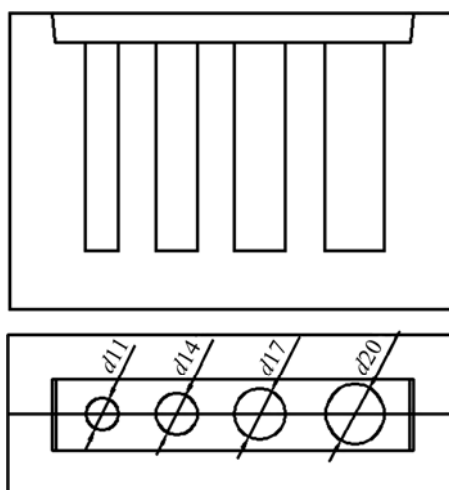


Fig. 4 Schematic diagram of copper mould for rapid cooling experiment (The bottom drawing is a top view)

The cooling rates of the positions about 10 mm apart from the bottom of each sample were simulated by the Flow-3D software. The simulated results are listed in Table 1. The cooling rates increase rapidly from 124.2 to 276.8 °C/s with the diameter decreasing from 20 mm to 11 mm. The optical microstructures of as-cast samples with different diameters and cooling rates are presented in Fig. 5. The sample in diameter of 20 mm (Fig. 5(a)) shows typical equilibrium solidified microstructure with finer eutectic than that of gravity cast alloy as shown in Fig. 3. A small amount of coarse α (Al) dendrites exist in

microstructure of sample in $d17$ mm as shown in Fig. 5(b). Furthermore, the amount of dendritic α (Al) phases increase with the increase of cooling rate (Fig. 5(c)). The non-equilibrium α (Al) phases tend to be rosette-like or fine dendrites phases (Fig. 5(d)) when the cooling rate reaches 276.8 °C/s. According to this experiment, the SC swash plate solidified with cooling rate about 218.4 °C/s would also cause the solidification of non-equilibrium dendritic α (Al).

Table 1 Cooling rate of samples simulated by Flow-3D software

Sample	Cooling rate/(°C·s ⁻¹)				SC after USV (690 °C)
	$d\ 20$	$d\ 17$	$d\ 14$	$d\ 11$	SC (760 °C)
Copper mould	124.2	152.1	196.4	276.8	
Swash plate					218.4

In the SC process, the pressure was imposed on the melt continuously after the mold-filling. Then more effective contact areas were formed for the reduction of the air gap between the melt and the die wall. Substantial increase in heat-transfer coefficients and greater cooling rates for the solidifying alloy could be obtained. LEE et al [16] studied the difference of thermal conductivity between conventional casting and SC process by forming 5083 Al alloy. In gravity die casting, the heat-transfer

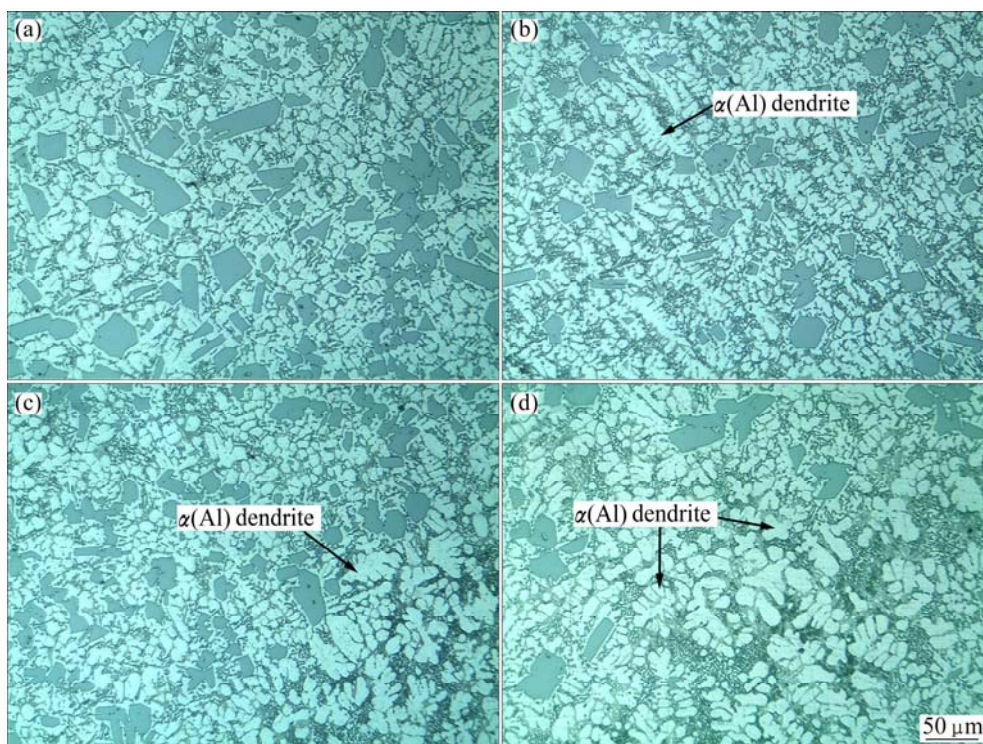


Fig. 5 Microstructures of Al-20% Si alloy formed in copper mold at pouring temperature of 760 °C with different diameters: (a) 20 mm; (b) 17 mm; (c) 14 mm; (d) 11 mm (Non-equilibrium α (Al) dendrites formed in the smaller samples are indicated by arrows.)

coefficient between 5083 Al alloy and the mold was $4.5 \text{ kW}/(\text{m}^2\cdot\text{K})$. Much higher heat-transfer coefficient about $125 \text{ kW}/(\text{m}^2\cdot\text{K})$ could be obtained in SC process under 100 MPa. Obviously, the cooling rate under SC condition for the solidifying alloy is much greater than that generated by conventional gravity casting. Generally, the cooling rates of both SC and die-casting are 3–5 times that of conventional gravity casting. The cooling rates of SC swash plate and semi-solid RSC swash plate simulated by the Flow-3D software are $218.4 \text{ }^\circ\text{C/s}$ and $250.4 \text{ }^\circ\text{C/s}$, respectively (Table 1). Therefore, it tends to form non-equilibrium solidified $\alpha(\text{Al})$ phase under such cooling rate condition as mentioned above. When Al–20%Si alloy solidified under pressure accompanied with greater cooling rate, the primary Si particles form firstly in the melt with the decrease of temperature. Then, micro area with low concentration of Si atoms forms around the solid–liquid interface of preformed Si particles. Generally, the zone of eutectics of Al–Si alloy is asymmetric tilting to Si side in Al–Si binary phase-diagram. When the under-cooled melt of hypereutectic Al–Si alloy solidifies under the eutectic temperature, it is easy to form single $\alpha(\text{Al})$ phase and grow into dendrite freely under rapid cooling condition. Dendritic $\alpha(\text{Al})$ phases tend to form under the eutectic temperature in SC parts as shown in Fig. 2. Finally, the remained melts with the composition near eutectic after the forming of dendritic $\alpha(\text{Al})$ phases, finish the solidification process with the growth of eutectic solidification. The formed eutectic microstructures are similar to that of the water quenched alloy because of the rapid cooling rate.

3.2 Effect of ultrasonic vibration on solidification of non-equilibrium $\alpha(\text{Al})$ phase

Figure 6 presents the typical optical microstructure of as-cast Al–20%Si alloy prepared by RSC with semi-solid slurry made by USV treatment. A large number of nearly spherical $\alpha(\text{Al})$ grains exist as shown in Fig. 6, compared with apparent $\alpha(\text{Al})$ dendrites of SC

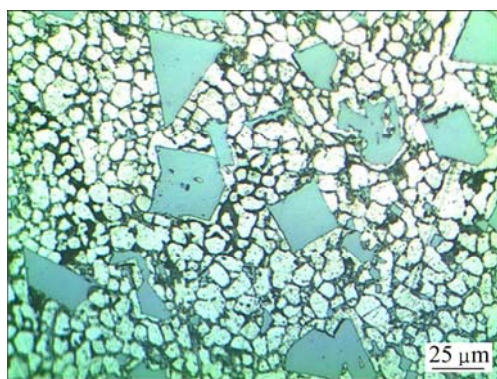


Fig. 6 Optical microstructure of semi-solid RSC Al–20%Si alloy after USV treatment

Al–20%Si alloy in Fig. 2. Both the morphology and the amount of $\alpha(\text{Al})$ phases formed by RSC are different from those solidified under rapid cooling rate. Non-equilibrium $\alpha(\text{Al})$ grains seem to exist independently rather than along with the primary Si particles. The round $\alpha(\text{Al})$ particles and Si phases are expected to be solidified respectively. Image analysis software was used to calculate the average volume fraction of $\alpha(\text{Al})$ phases in SC and RSC Al–20%Si alloy. The volume fraction of $\alpha(\text{Al})$ grains in RSC Al–20%Si alloy is 49.4%, which is 1.36 times as that of SC Al–20%Si alloy (35.3%).

Two kinds of phenomena named as cavitation and acoustic streaming would be produced by the application of USV in the melt. Acoustic cavitation is characterized as focusing and releasing the acoustic energy in a short time. When cavitation bubbles collapse, high temperature over 5000 K and high pressure about 1 GPa would be generated in a very short time and small space in fine cavitation bubbles. Additionally, strong shock wave and micro jet with the speed up to 400 km/h would be accompanied [17]. The high pressure in some melt of local area was imposed by USV, which would make the phase diagram changed. The Si content of eutectic point moves to 17%Si and the eutectic temperature rises to about $640 \text{ }^\circ\text{C}$ [15]. Some micro areas of this hypereutectic Al–Si alloy melt could transfer to eutectic or even hypoeutectic melt with the effect of USV. Based on the Clausius–Clapeyron equation, the pressure dependence on the melting point was calculated to increase by $6.2 \text{ }^\circ\text{C}/0.1 \text{ GPa}$ for the melting point of aluminum and $-4.1 \text{ }^\circ\text{C}/0.1 \text{ GPa}$ for the melting point of silicon [18]. The $\alpha(\text{Al})$ grains could stably exist as a solid state under high pressures, though a liquid state at ambient pressure. Hence, non-equilibrium $\alpha(\text{Al})$ phase would form as the primary solidified phase above the eutectic temperature.

It has been reported that the solute concentration in crystal front decreased significantly with the combined effects of acoustic streaming and micro-flow by USV treatment [19]. The degree of constitutional under-cooling is also decreased with the decrease of boundary layer thickness in crystal front. In the following solidification process, the preformed $\alpha(\text{Al})$ nuclei tend to grow into non-dendrite for the uniform distributed fields of temperature and solute in front of solidifying crystal. The remnant melt is cooled below the eutectic temperature accompanying the gradual forming of primary Si particles and non-equilibrium $\alpha(\text{Al})$ grains. Obviously, the non-equilibrium $\alpha(\text{Al})$ phases of semi-solid SC Al–20%Si alloy after USV treatment consist of α_1 grains which formed above the eutectic temperature and α_2 dendrites formed under eutectic temperature as shown in Fig. 7(a).

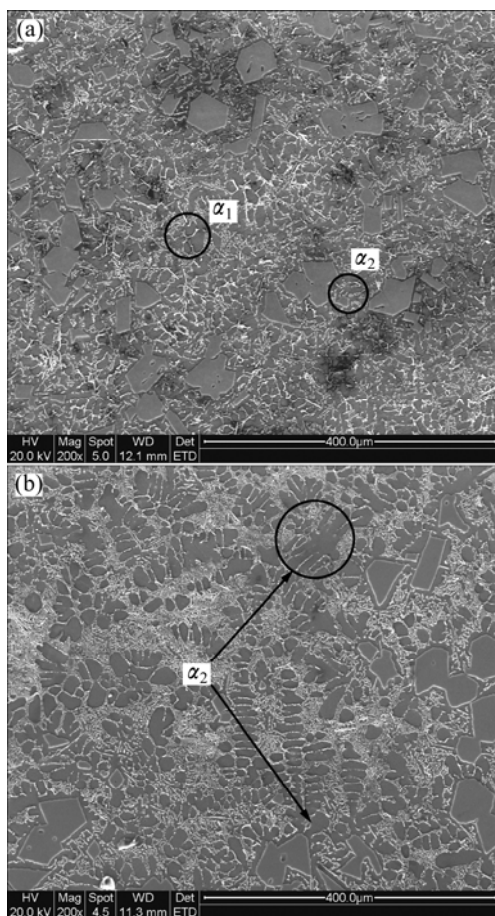


Fig. 7 SEM images of as-cast Al–20%Si alloy: (a) Semi-solid RSC at 690 °C; (b) SC at 760 °C

It is expected that the Si contents of α_1 and α_2 are different from each other at different forming temperatures. The EDS analysis results of Si content in non-equilibrium $\alpha(\text{Al})$ phases are presented in Fig. 8 and Table 2. The Si content of α_1 and α_2 in RSC Al–20% Si alloy are 2.98% and 2.03% respectively, while that of dendritic α_2 in SC Al–20% Si alloy is 2.34%. Obviously, the Si content of non-equilibrium solidified $\alpha(\text{Al})$ phase of both semi-solid RSC and SC alloys is higher than that of $\alpha(\text{Al})$ eutectic formed in conventional gravity cast alloy, which was about 1.84% [19]. The main reason is that the rapid cooling rate produced by SC process contributed to form supersaturated $\alpha(\text{Al})$ solid solution. Supersaturated α phase with a higher Si content could be obtained by the semi-solid RSC alloy for the non-equilibrium $\alpha(\text{Al})$ grains formed above the eutectic temperature.

3.3 Characteristics of primary Si in Al–20%Si alloy formed by semi-solid squeeze casting

Figure 9 shows the optical microstructures of SC and semi-solid RSC Al–20%Si alloys respectively. Coarse and polygonal Si particles exist in SC alloy, and obvious segregation can be observed under such

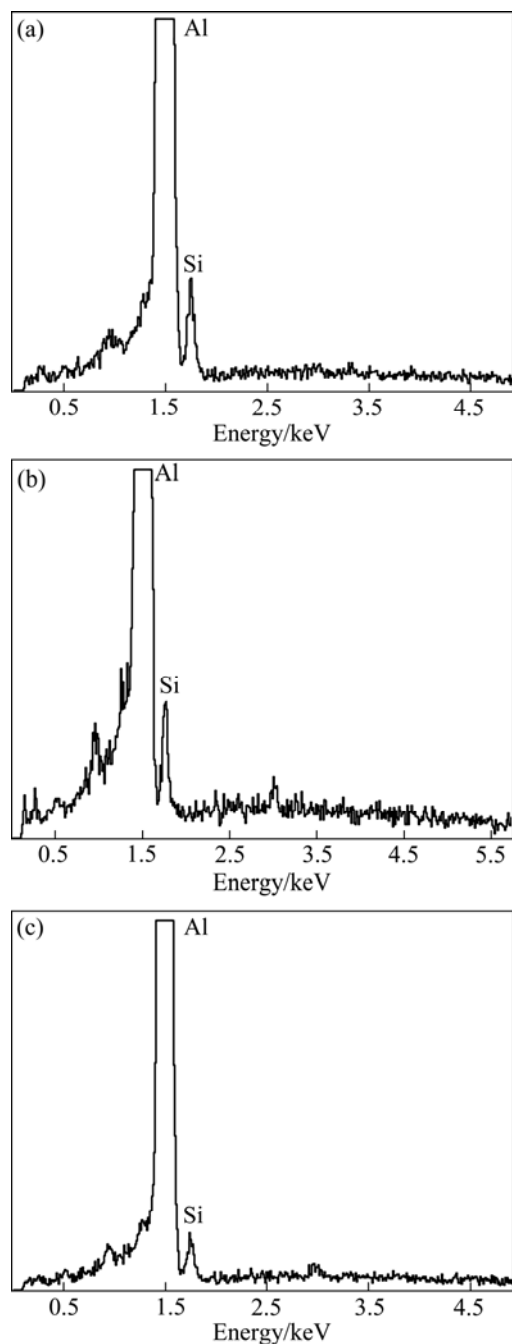


Fig. 8 EDS analysis of Si atom of non-equilibrium $\alpha(\text{Al})$: α_1 (a) and α_2 (b) of semi-solid RSC alloy; (c) α_2 of SC alloy

Table 2 Mass fraction of Si atom in $\alpha(\text{Al})$ phases of Al–20%Si alloy by EDS (mass fraction, %)

Semi-solid RSC		SC	Gravity casting
α_1	α_2	α_2	$\alpha(\text{Al})$ (eutectic)
2.98	2.03	2.34	1.84

condition. In contrast, with USV treatment, the primary Si particles are refined significantly with favorable morphology modification, most of which are granular or even spherical grains with more uniform distribution.

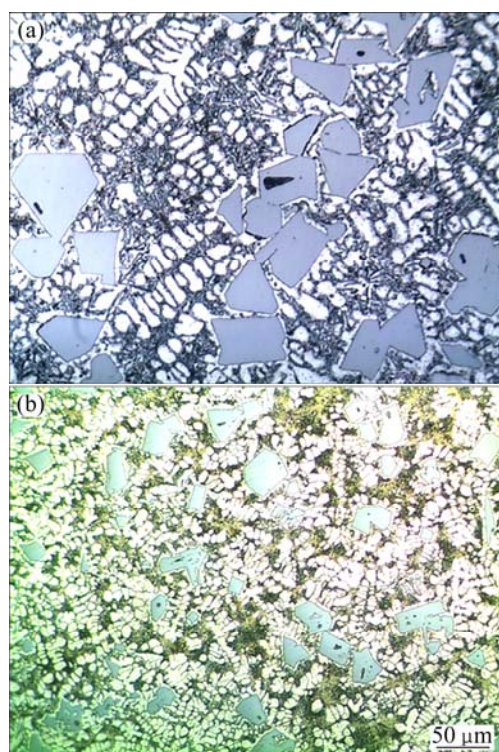


Fig. 9 Optical images of as-cast Al-20%Si alloy, showing morphology of Si particles: (a) SC at 760 °C; (b) Semi-solid RSC at 690 °C

The image analysis software was used to quantitatively analyze the primary Si difference between SC and semisolid RSC Al-20%Si alloy. The average particle diameter and volume fraction of primary Si particles were calculated respectively, as shown in Table 3. The average particle diameter of primary Si particles in SC Al-20%Si alloy is 42.9 μm , and the volume fraction is 21.2%. While in semi-solid RSC alloy, the average particle diameter is 24.3 μm , and the volume fraction is 11.1%, which are decreased by 43% and 47.8%, respectively, than those of SC Al-20%Si alloy. Statistical analysis by this software presented that the shape factor of primary Si of semi-solid RSC alloy was about 0.52, higher than that about 0.43 of SC alloy. Obviously, semi-solid SC alloy with USV treatment got more spherical primary Si particles.

Table 3 Average particle diameter and volume fraction of primary Si particles

Average particle diameter/ μm		Volume fraction/%	
SC	Semi-solid RSC	SC	Semi-solid RSC
42.9	24.3	21.2	11.1

USV has the effects of refining the microstructure which is supposed to play the role of promoting nucleation and fragmentation of grains by cavitation and acoustic streaming [8]. Moreover, the greater cooling rate, which was caused by the lower forming temperature

of semi-solid RSC process at 690 °C, contributed to finer microstructure and modified primary Si particles.

The volume fraction of primary Si is expected to have the relationship with different forming processes. The volume fraction of primary Si of a multi-element Al-20%Si alloy cooled in 1 °C/s was investigated by YAMAGATA et al [4]. The volume fraction of primary Si was 21.6% in his study. As can be seen from Table 3, the volume fraction of primary Si in SC Al-20%Si alloy is similar to the finding of YAMAGATA et al [4]. But the semi-solid RSC Al-20%Si alloy presents much lower volume fraction of primary Si, as just 11.1%. This is mainly because that the primary Si particles of SC Al-20%Si alloy sustain to form until the melt reaches the eutectic temperature near 577 °C. The SC Al-20%Si alloy shows the same forming process as conventional casting as studied by YAMAGATA et al [4]. While the eutectic temperature of some micro areas under USV treatment would increase, even to 640 °C, and non-equilibrium $\alpha(\text{Al})$ grains are formed simultaneously with the formation of primary Si particles. As a result, the forming temperature range of primary Si is decreased greatly with decreasing from 694–577 °C to 694–640 °C, leading to lower volume fractions of primary Si in semi-solid RSC Al-20%Si alloy with USV treatment. ZHONG et al [19] showed that the solid solubility of Si atoms in $\alpha(\text{Al})$ matrix increased from 1.84% to 2.79%. As a result, it also caused the decrease of volume fraction of primary Si particles.

4 Conclusions

1) A swash plate of Al-20Si-2Cu-0.4Mg-1Ni alloy (Al-20%Si alloy) was made in a relatively lower forming temperature with rheo-squeeze casting (RSC) process after ultrasonic vibration. Non-equilibrium $\alpha(\text{Al})$ phases are discovered in the microstructure of this alloy. The volume fraction of non-equilibrium $\alpha(\text{Al})$ grains in semi-solid RSC Al-20%Si alloy is 49.4%, which is 1.36 times that of conventional squeeze casting Al-20%Si alloy.

2) A small amount of non-equilibrium $\alpha(\text{Al})$ dendrites in Al-20%Si alloys could form when the cooling rate is higher than 150 °C/s or so approved by a copper-mould experiment. Lots of $\alpha(\text{Al})$ phases present in fine dendrite or rosette shape under the cooling rate of 218 °C/s. The rapid cooling rate mainly contributes to the formation of non-equilibrium $\alpha(\text{Al})$ dendrites in squeeze cast Al-20%Si alloy.

3) The formation of non-equilibrium $\alpha(\text{Al})$ particles of semi-solid RSC Al-20% Si alloy with ultrasonic vibration treatment is promoted by the effects of acoustic cavitation. Locally high pressure generated by acoustic cavitation makes the formation of $\alpha(\text{Al})$ phases above eutectic temperature.

4) The average particle diameter and the volume fraction of primary Si particles of the swash-plate by rheo-squeeze casting are 24.3 μm and 11.1% respectively, which are smaller than those of conventional squeeze casting alloys.

References

- [1] CHEN C, LIU Z X, REN B, WANG M X, WENG Y G, LIU Z Y. Influences of complex modification of P and RE on microstructure and mechanical properties of hypereutectic Al–20Si alloy [J]. Transactions of Nonferrous Metals Society of China, 2007, 17(2): 301–306.
- [2] WU S S, TU X L, FUKUDA Y, KANNO T, NAKAE H. Modification mechanism of hypereutectic Al–Si alloy with P–Na addition [J]. Transactions of Nonferrous Metals Society of China, 2003, 13(6): 1285–1289.
- [3] YAMAGATA H, KASPRZAK W, ANIOLEK M, KURITA H, SOKOLOWSKI J H. Thermal and metallographic characteristics of the Al–20%Si high-pressure die-casting alloy for monolithic cylinder blocks [J]. Journal of Materials Processing Technology, 2008, 199: 84–90.
- [4] YAMAGATA H, KASPRZAK W, ANIOLEK M, KURITA H, SOKOLOWSKI J H. The effect of average cooling rates on the microstructure of the Al–20% Si high pressure die casting alloy used for monolithic cylinder blocks [J]. Journal of Materials Processing Technology, 2008, 203: 333–341.
- [5] BIROL Y. Semisolid processing of near-eutectic and hypereutectic Al–Si–Cu alloys [J]. Journal of Materials Science, 2008, 43: 3577–3581.
- [6] LASHKARI O, AJERSCH F, CHARETTE A, CHEN X. Microstructure and rheological behavior of hypereutectic semi-solid Al–Si alloy under low shear rates compression test [J]. Materials Science and Engineering A, 2008, 492: 377–382.
- [7] GHOMASHCHI M R, VIKHROV A. Squeeze casting: An overview [J]. Journal of Materials Processing Technology, 2000, 101: 1–9.
- [8] WU S S, ZHAO J W, ZHANG L P, AN P, MAO Y W. Development of non-dendritic microstructure of aluminum alloy in semi-solid state under ultrasonic vibration [J]. Solid State Phenomena, 2008, 141–143: 451–456.
- [9] KANG Yong-lin, YANG Liu-qing, SONG Ren-bo, ZHANG Fan, TAO Tao. Study on microstructure–processing relationship of a semisolid rheocasting A357 aluminum alloy [J]. Solid State Phenomena, 2008, 141–142: 137–162.
- [10] GUAN Ren-guo, WANG Chao, SHANG Jian-hong, XING Zhen-huan. Semisolid metal forming by novel sloping plate process [J]. Transactions of Nonferrous Metals Society of China, 2006, 16(s): s1265–s1269.
- [11] WU S S, YOU Y, AN P, KANNO T, NAKAE H. Effect of modification and ceramic particles on solidification behavior of aluminum-matrix composites [J]. Journal of Materials Science, 2002, 37: 1855–1860.
- [12] MAO W M, ZHENG Q, ZHU D P. Rheo-squeeze casting of semi-solid A356 aluminum alloy slurry [J]. Transactions of Nonferrous Metals Society of China, 2010, 20(9): 1769–1773.
- [13] ZHAO J W, WU S S, AN P, MAO Y W. Preparation of semi-solid slurry of hypereutectic Al–Si alloy by ultrasonic vibration [J]. Solid State Phenomena, 2008, 141–143: 767–771.
- [14] ZHONG G, WU S S, JIANG H W, AN P. Effects of ultrasonic vibration on the iron-containing intermetallic compounds of high silicon aluminum alloy with 2% Fe [J]. Journal of Alloys and Compounds, 2010, 492: 482–487.
- [15] YU X F, ZHANG G Z, WANG X Y, GAO Y Y, JIA G L, HAO Z Y. Non-equilibrium microstructure of hyper-eutectic Al–Si alloy solidified under superhigh pressure[J]. Journal of Materials Science, 1999, 34: 4149–4152.
- [16] LEE J H, KIM H S, HONG S I, WON C W, CHO S S, CHUN B S. Effect of die geometry on the microstructure of indirect squeeze cast and gravity die cast 5083 wrought Al alloy and numerical analysis of the cooling behavior [J]. Journal of Materials Processing Technology, 1999, 96: 188–197.
- [17] ESKIN G I. Ultrasonic treatment of light alloy melts [M]. Russia: Overseas Publishers Association, 1998: 1–18.
- [18] LU S L, WU S S, LIN C, HU Z Q, AN P. Preparation and rheocasting of semisolid slurry of 5083 Al alloy with indirect ultrasonic vibration process [J]. Materials Science and Engineering A, 2011, 528: 8635–8640.
- [19] ZHONG G, WU S S, JIANG H W, SHA M, AN P. Effects of ultrasonic vibration treatment on microstructure of heat-resistant Al–Si alloy [J]. Advanced Materials Research, 2009, 79–82: 1523–1526.

超声半固态流变挤压成形 Al–20Si–2Cu–0.4Mg–1Ni 合金的组织特征

吴树森¹, 钟 鼓¹, 安 萍¹, 万 里¹, 中江秀雄²

1. 华中科技大学 材料成形与模具技术国家重点实验室, 武汉 430074;

2. 早稻田大学 材料科学与工程系, 东京 169, 日本

摘 要: 通过超声振动半固态流变挤压铸造工艺制造汽车空调压缩机铝硅合金斜盘零件, 研究合金的组织特征。发现在 Al–20Si–2Cu–0.4Mg–1Ni 合金的组织中, 除了通常具有的初晶 Si 和 $\alpha(\text{Al})+\beta\text{-Si}$ 共晶相之外, 还有非平衡 $\alpha(\text{Al})$ 颗粒或枝晶。挤压铸造过程中的较快的冷却速度而非压力是非平衡 $\alpha(\text{Al})$ 相形成的主要原因。在半固态浆料的制备过程中, 超声振动的声压作用能促进非平衡 $\alpha(\text{Al})$ 相在共晶温度以上生成, 并生长为非枝晶颗粒。超声处理的过共晶 Al–Si 合金中的非平衡 $\alpha(\text{Al})$ 相由共晶温度以上生成的圆形 $\alpha(\text{Al})$ 晶粒和少量共晶温度以下生成的细小 $\alpha(\text{Al})$ 枝晶构成。由于超声振动的作用使 $\alpha(\text{Al})$ 基体中的 Si 的固溶度增加, 并使初晶 Si 的形成温度降低, 组织中初晶 Si 颗粒的体积分数显著降低。流变挤压斜盘中的初晶 Si 颗粒的平均直径和体积率分别为 24.3 μm 和 11.1%。

关键词: Al–Si 合金; 过共晶; 超声振动; 挤压铸造; 非平衡 $\alpha(\text{Al})$; 半固态浆料

(Edited by LI Xiang-qun)